


Article

Ignition of Wood-Based Boards by Radiant Heat

Iveta Marková ^{1,*}, Martina Ivaničová ², Linda Makovická Osvaldová ¹ , Jozef Harangózo ² and Ivana Tureková ²

¹ Department of Fire Engineering, Faculty of Security Engineering, University of Žilina, Univerzitná 1, 010 26 Zilina, Slovakia

² Constantine the Philosopher University in Nitra, Tr. A. Hlinku 1, 949 74 Nitra, Slovakia

* Correspondence: iveta.markova@uniza.sk; Tel.: +421-41-513-6799

Abstract: Particleboards (PB) and oriented strand boards (OSB) are commonly used materials in building structures or building interiors. The surface of boards may hence become directly exposed to fire or radiant heat. The aim of this paper is to evaluate the behaviour of uncoated particleboards and OSB exposed to radiant heat. The following ignition parameters were used to observe the process of particleboard and OSB ignition: heat flux intensity (from 43 to 50 kW.m⁻²) and ignition temperature. The time-to-ignition and mass loss of particleboards and OSB with thicknesses of 12, 15 and 18 mm were monitored and compared. The experiments were conducted on a modified device in accordance with ISO 5657: 1997. Results confirmed thermal degradation of samples. Heat flux had a significant effect on mass loss (burning rate) and time-to-ignition. OSB had higher ignition time than particleboards and the thermal degradation of OSB started later, i.e., at a higher temperature than that of particleboards, but OSB also had higher mass loss than particleboards. The samples yielded the same results above 47 kW.m⁻². Thermal analysis also confirmed a higher thermal decomposition temperature of OSB (179 °C) compared to particleboards (146 °C). The difference in mass loss in both stages did not exceed 1%.



Citation: Marková, I.; Ivaničová, M.; Osvaldová, L.M.; Harangózo, J.; Tureková, I. Ignition of Wood-Based Boards by Radiant Heat. *Forests* **2022**, *13*, 1738. <https://doi.org/10.3390/f13101738>

Academic Editors: Réh Roman, Petar Antov, Ľuboš Krišťák, Muhammad Adly Rahandi Lubis and Seng Hua Lee

Received: 23 September 2022

Accepted: 18 October 2022

Published: 20 October 2022

Publisher's Note: MDPI stays neutral with regard to jurisdictional claims in published maps and institutional affiliations.



Copyright: © 2022 by the authors. Licensee MDPI, Basel, Switzerland. This article is an open access article distributed under the terms and conditions of the Creative Commons Attribution (CC BY) license (<https://creativecommons.org/licenses/by/4.0/>).

Keywords: particleboard; OSB; heat release; time-to-ignition; mass loss

1. Introduction

The production of wood-based boards encompasses the utilization of wood of lower quality classes [1–4] and obtaining suitable materials with improved physical and mechanical properties [5–10]. Properties of particleboards (PB) are described in detail in the work of [11,12]. The oriented strand boards (OSB) belong to this product group, but they are also considered an input material in the furniture and construction industries [9,13–15]. A description of OSB in terms of their preparation and properties is defined in the work of [16,17]. These materials are also analysed within the scope of insulation materials [18–21]. They are a part of sandwich panels in low-energy houses [22–25]. They are typically used as an interior sheathing material [26] or furniture [27–30]. Research on the fire resistance of the mentioned materials is also rich [31–35].

Large-size wood-based materials form the largest percentage of wood material in timber houses [36–38]. These materials can be directly exposed to fire [39–41] or the effect of radiant heat [42,43]. Thermal degradation and potentially even ignition of wood-based boards are caused by the action of the ignition source [41–48]. These processes are affected by both the combustible material and the environment in which it is located [49,50]. The ignition process cannot be characterized by a single property [51]. Rantuch et al. [52] used ignition parameters to define the term ignition. Two of these ignition parameters (critical heat flux and ignition temperature) are used here to compare OSB and PB with thicknesses of 12, 15 and 18 mm. This article presents the differences in the results of the research between PB and OSB due to the influence of external heat flux.

Ignition is the ability of a sample to ignite under the action of an external thermal initiator and under defined test conditions, according to [53]. According to ISO 3261 [54],

it is the ability of a material to ignite. The process of ignition is characterized by the time-to-ignition of a sample, which depends on the ignition temperature, thermal properties of materials, sample conditions (size, humidity, orientation) and critical heat flux [55]. Definition of “ignition temperature” can be interpreted as the minimum temperature to which the air must be heated so that the sample placed in the heated air environment ignites, or the surface temperature of the sample just before the ignition point [56–58].

Separate attention is paid to the issue of simulating the ignition of wood under external heat flux from calculations of ignition parameters [59,60]. A prediction model presented in Chen et al.’s paper [61] studies the pyrolysis and ignition time of wood under external heat flux. The solution of the model provides the temperature at each point of the solid and the local solid conversion, and the time-to-ignition of the wood is predicted with the solution of surface temperature [62]. Chen et al. [61] obtained good agreement between experimental and theoretical results.

The aim of this paper is to evaluate the behaviour of uncoated particleboards and OSB exposed to radiant heat. The significant influence of board density and thickness on time-to-ignition and mass loss of PB and OSB samples is monitored and observed. At the same time, the difference in the thermal degradation of PB and OSB samples is sought by comparing the results between time-to-ignition and mass loss of PB and OSB samples.

2. Materials and Methods

2.1. Experimental Samples

Particleboards (PB) and OSB with thicknesses of 12, 15 and 18 mm (Figure 1a) were used as samples. Selected thicknesses correspond to those typically used in the construction and insulation of houses, in the construction of ceilings, soffits, partitions, etc. The samples were sourced from the company BUČINA DDD, Zvolen, under the product name Particleboard raw unsanded (Table 1). These particleboards contain softwood strands, mainly spruce, and a urea–formaldehyde adhesive mixture [63].

The samples of oriented strand boards were obtained from the company Kronospan-Jihlava, under product name OSB/3 SUPERFINISH ECO (Figure 1b), without surface treatment. These OSB are multi-layered boards made of flat wood chips of a specific shape and thickness. The chips in the outer layers are oriented parallel to the length or width of the board, the chips in the middle layers may be oriented randomly or generally perpendicular to the lamellae of the outer layers. They are bonded with melamine formaldehyde resin and PMDI, and they are flat-pressed. The boards contain mainly a mixture of different softwood species [64].

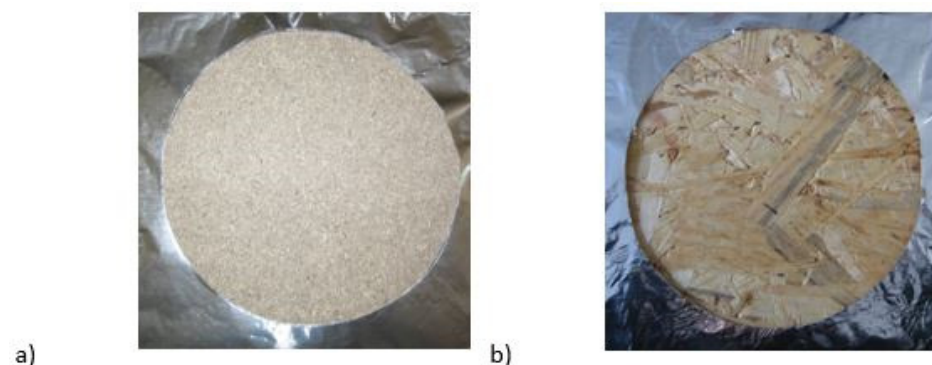


Figure 1. Example of experimental samples prepared in accordance with ISO 5657 [65]: (a) particleboard (PB); (b) OSB.

The samples of OSB were cut to specific dimensions (165×165 mm) according to ISO 5657: 1997 [65]. Selected sheet board materials were stored at a specific temperature ($23 \text{ }^\circ\text{C} \pm 2 \text{ }^\circ\text{C}$) and relative humidity ($50 \pm 5\%$).

There were tested air-conditioned samples, because the change in moisture will affect the thermal parameters of the samples and subsequently the thermal processes [16,66]. The

density of samples (Table 1) was determined according to EN 323: 1996 [67]. The remaining parameters were obtained from the safety data sheets (Table 2).

Table 1. The density of PB and OSB samples according to EN 323: 1996 [67].

Samples	Designation	Density ($\text{kg}\cdot\text{m}^{-3}$) for Thickness (mm)		
		12	15	18
Particleboard (PB)	PB	690 ± 9.8	713 ± 9.7	644 ± 10.1
Oriented Strand Boards (OSB)	OSB	562 ± 7.9	570 ± 12.1	569 ± 12.8

Table 2. Physical and chemical properties and fire-technical characteristics of particleboards and OSB with thicknesses of 10–18 mm.

Parameters	PB [64]	OSB [63]
Density ($\text{kg}\cdot\text{m}^{-3}$)	665	630
Moisture (%)	5	5
Swelling (%)	3.5	15
Thermal conductivity ($\text{W}\cdot\text{m}^{-2}\cdot\text{K}^{-1}$)	0.10–0.14	0.13
Specific heat ($\text{J}\cdot\text{kg}^{-1}\cdot\text{K}^{-1}$) [67]	-	1460–1470
Formaldehyde content ($\text{mg}\cdot 100\text{ g}^{-1}$)	6.5	8
Flame spread rating ($\text{mm}\cdot\text{min}^{-1}$)	-	83.8
Reaction to fire	D-s1, d0	

2.2. Methodology

2.2.1. Determination of Mass Loss and Time-to-Ignition

The measuring instrument was calibrated, and heat flux values used for selected samples were logged in Tureková et al. [68,69].

Time-to-ignition and mass loss were determined for the selected level of heat flux density and thickness of the sheet board materials according to a modified procedure based on ISO 5657: 1997 [65]. This modification included a change of the igniter. The ignition was caused only by heat flux, without the use of an open flame (Figure 2).

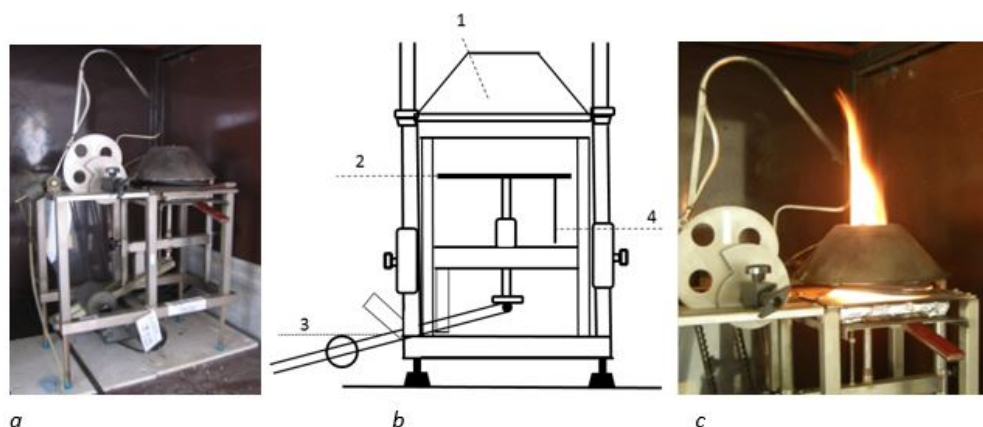


Figure 2. Scheme of the equipment for determination of flammability of materials at radiant heat flux of $10\text{--}50\text{ kW}\cdot\text{m}^{-2}$ according to ISO 5657: 1997 [65]. (a) Real test equipment and equipment scheme. (b) Scheme of the used equipment with description of components: 1—heating cone, 2—board for sample, 3—movable arm, 4—connection point for recording experimental data. (c) Detailed look at the burning of the particleboard sample with 18 mm thickness in 100 s.

The samples were placed horizontally and exposed to a heat flux of 43 to $50\text{ kW}\cdot\text{m}^{-2}$ by an electrically heated cone calorimeter. Orientation experiments determined the minimum heat flux required to maintain flame combustion. Time-to-ignition and mass loss were

monitored in the interval of 43 to 50 kW.m⁻² at each thickness of the sheet board material in a series of five repetitions.

The factors which affect time-to-ignition and mass loss are type of sample, board thickness and heat flux density. The obtained results of the ignition and mass loss temperatures were statistically evaluated by statistics. The following factors were used: mixture samples, board thickness (12, 15 and 18 mm) and heat flux density (from 43 to 50 kW.m⁻²).

2.2.2. Thermal Analysis (Thermogravimetry TGA) of PB and OSB

This analytical method was chosen as the weight of the analysed samples in milligrams. These methods are used in observations and comparison of thermal decomposition of samples, and in the research of the changes and conditions of the chemical reaction course. Thermogravimetry (TGA) studies the course of both thermolysis and polymer burning and records the changes in the weight of the heated sample. The sample was stabilized for 24 h under standard conditions; the test was conducted on a Mettler TA 3000 with a TC 10A processor and TG 50 thermogravimetric weights module in the air and flow rate of 200 mL.min⁻¹. The heat increased at a rate of 10 °C.min⁻¹. The test was carried out up to a temperature of 700 °C. The samples for TGA were specifically prepared by disintegration, and the weight of the OSB sample was 10.225 mg and PB was 10.543 mg.

3. Results and Discussion

The minimum value of radiant heat flux for particleboards and OSB was approximately 43 kW.m⁻². This value represented the critical heat flux for the selected samples. The maximum value of the radiant heat flux, to which the selected sheet board materials were exposed, was 50 kW.m⁻². The heat flux was gradually increased by 1 kW.m⁻² (Table 3).

Table 3. Time-to-ignition and mass loss of samples with different thicknesses using heat fluxes from 43 to 50 kW.m⁻² at a distance of 20 mm.

Radiant Heat Flux (kW.m ⁻²)	Thickness (mm)	PB		OSB	
		Time-to-Ignition (s)	Mass Loss Δm (%)	Time-to-Ignition (s)	Mass Loss Δm (%)
43	12	89.0 ± 5.215	17.108 ± 0.520	107.4 ± 32.920	19.018 ± 0.742
	15	92.6 ± 3.441	14.604 ± 0.375	172.8 ± 68.271	16.528 ± 1.103
	18	117.0 ± 5.513	13.198 ± 0.173	170.0 ± 19.279	12.436 ± 0.402
44	12	80.0 ± 5.366	17.594 ± 0.409	80.80 ± 14.372	20.188 ± 1.210
	15	86.4 ± 4.882	15.452 ± 0.355	108.0 ± 31.093	16.092 ± 0.885
	18	102.8 ± 4.308	13.754 ± 0.239	140.0 ± 31.698	13.256 ± 0.745
45	12	78.2 ± 0.748	17.96 ± 0.301	100.2 ± 21.673	20.870 ± 0.889
	15	84.4 ± 2.057	15.27 ± 0.294	86.4 ± 10.442	17.026 ± 0.541
	18	92.2 ± 2.481	13.87 ± 0.286	111.2 ± 24.235	13.716 ± 0.303
46	12	71.6 ± 1.624	18.406 ± 0.522	84.4 ± 9.002	21.868 ± 0.879
	15	76.0 ± 2.280	15.714 ± 0.290	93.4 ± 21.767	17.272 ± 0.647
	18	89.0 ± 7.974	13.776 ± 0.565	98.8 ± 12.592	13.504 ± 0.228
47	12	66.4 ± 2.870	18.91 ± 0.288	71.0 ± 8.671	22.026 ± 0.908
	15	73.8 ± 0.797	16.23 ± 0.363	67.08 ± 5.403	17.500 ± 0.455
	18	75.6 ± 3.720	14.48 ± 0.339	103.6 ± 18.391	13.818 ± 0.266
48	12	64.0 ± 1.490	19.11 ± 0.338	58.60 ± 5.953	23.206 ± 0.505
	15	69.4 ± 1.959	16.27 ± 0.373	63.40 ± 7.116	18.366 ± 0.910
	18	75.0 ± 2.000	14.65 ± 0.225	77.60 ± 25.881	14.222 ± 0.826
49	12	60.6 ± 2.241	19.75 ± 0.439	65.0 ± 11.436	23.578 ± 0.858
	15	66.0 ± 2.283	16.59 ± 0.333	62.20 ± 3.2497	18.764 ± 0.571
	18	67.2 ± 1.166	15.17 ± 0.131	63.20 ± 3.187	14.678 ± 0.899
50	12	59.8 ± 2.638	19.91 ± 0.415	56.80 ± 2.039	24.302 ± 0.814
	15	64.4 ± 2.497	16.5 ± 0.335	59.40 ± 5.607	19.402 ± 0.586
	18	66.8 ± 2.093	15.94 ± 0.945	60.20 ± 5.741	14.846 ± 1.033

The sample was placed horizontally under the cone calorimeter and exposed to selected heat fluxes which led to gradual thermal degradation and generation of flammable gases. Thermal degradation (Figure 3) is manifested by mass loss (Table 3). Ignition occurs when the critical temperature is reached [69]. Time-to-ignition was recorded, while considering only the permanent ignition of the surface of the analysed sample when exposed to a selected level of heat flux density. The carbonized residue (Figure 4) remained on the surface which has been exposed to radiant heat [70–73], which proves the thermal insulation properties of the particleboard and OSB [25].

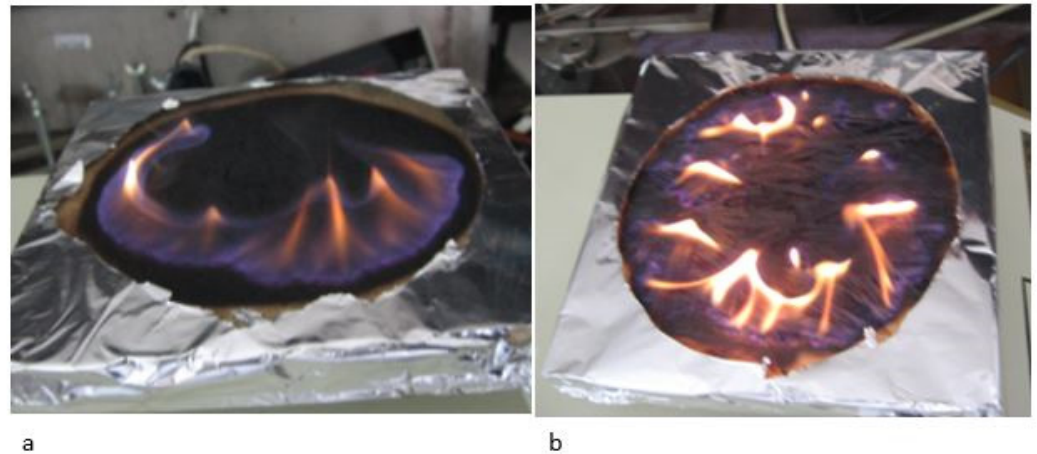


Figure 3. (a) Burning process of particleboard samples with 15 mm thickness after their ignition by radiant heat at $48 \text{ kW}\cdot\text{m}^{-2}$ in 80 s; (b) OSB sample with 15 mm thickness during experiment in 80 s at $48 \text{ kW}\cdot\text{m}^{-2}$.

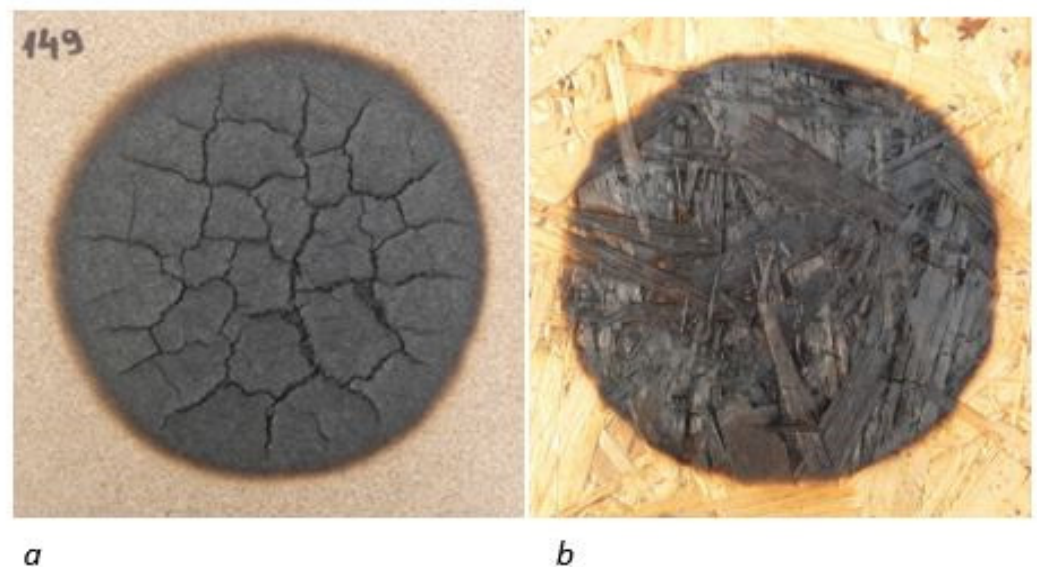
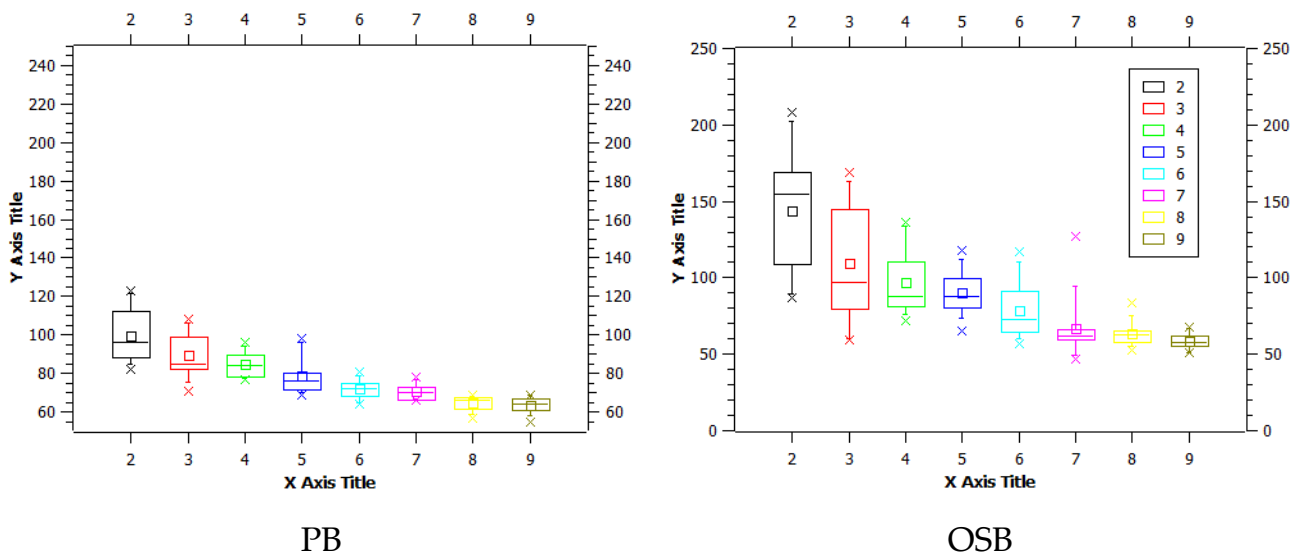
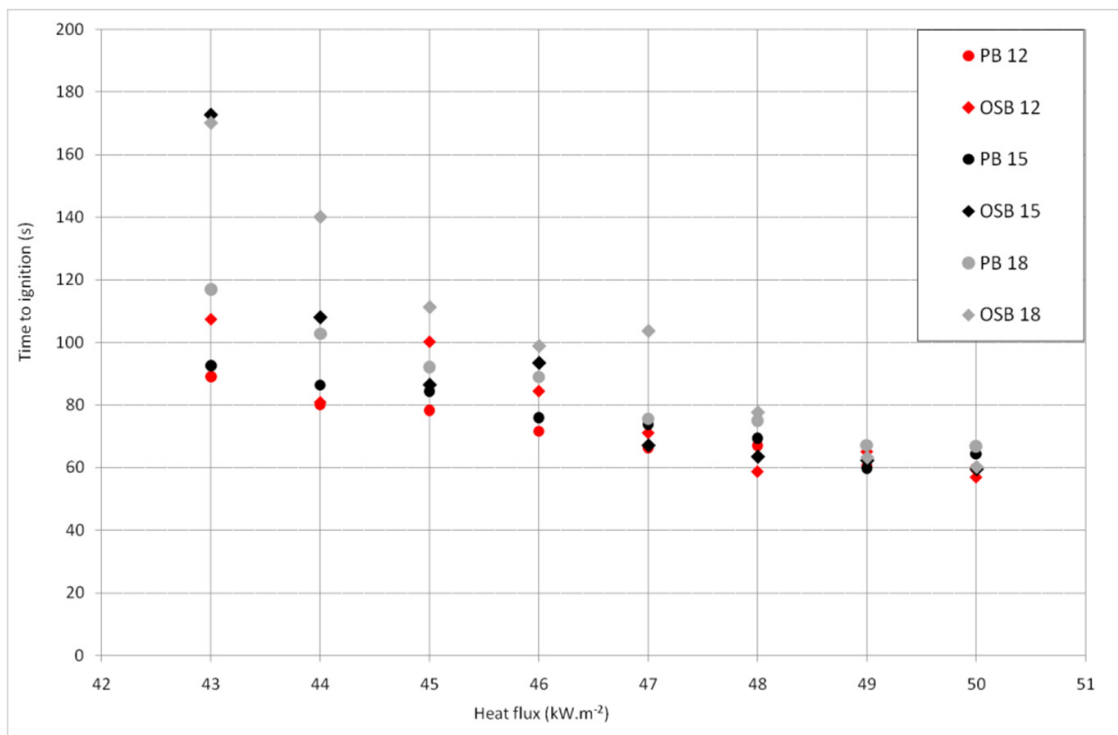


Figure 4. Cooled samples 10 min after the end of the experiment, sample thickness of 18 mm: (a) PB; (b) OSB.

Time-to-ignition of particleboard and OSB samples of the same thickness (Figure 4) differed in experiments with lower heat flux values, i.e., at 43 to $46 \text{ kW}\cdot\text{m}^{-2}$. Particleboards and OSB with thicknesses of 12 and 15 mm had the same time-to-ignition values starting from $47 \text{ kW}\cdot\text{m}^{-2}$ (Figure 4 and Table 1). Samples of particleboard and OSB with a thickness of 18 mm showed the same time stamps starting from $48 \text{ kW}\cdot\text{m}^{-2}$ (Figure 5).

In comparison with OSB, particleboards generally showed lower time-to-ignition values. The cause can be found in the board structure. OSB consist of larger wood chips compared to particleboards.

The box plot graph for time-to-ignition OSB and PB samples shows the dispersion of the obtained data (Figure 5c). PB samples, in all thicknesses, have comparable results (in Figure 5c), marked with the numbers 2 as PB 12, 4 as PB 15 and 6 as PB 18. The above matrix presents the data obtained from heat flux 43 to 50 kW.m⁻². It confirms the fact that the thickness of the sample does not have a significant influence on time-to-ignition for PB samples. OSB samples show a significant dispersion of the obtained data and confirm the ratio with increasing heat flux; the ignition time is shortened (see also in Figure 5a).



(a)

Figure 5. Cont.

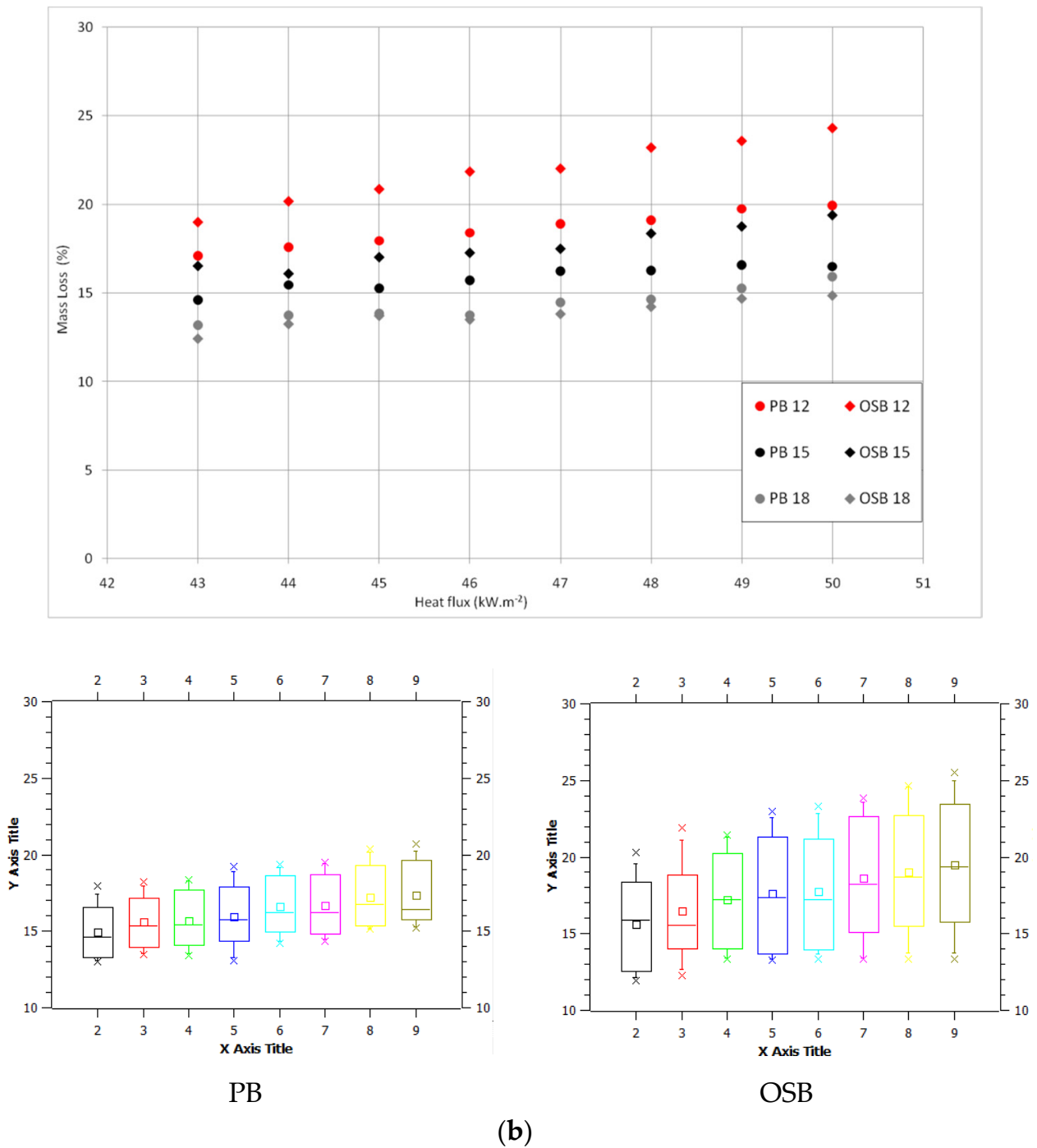


Figure 5. Comparison of time-to-ignition and mass loss values of particleboards and OSB depending on the heat flux values. (a) Comparison of time-to-ignition results with box graph, where X Axis is heat flux 43–50 kW.m⁻² and Y Axis is time-to-ignition for PB and OSB samples. (b) Comparison of mass loss results with box graph, where X Axis is heat flux 43–50 kW.m⁻² and Y Axis is mass loss for PB and OSB samples. Legends: PB 12—PB samples with 12 mm thickness, PB 15—PB samples with 15 mm thickness, PB 18—PB samples with 18 mm thickness, OSB 12—OSB samples with 12 mm thickness, OSB 15—OSB samples with 15 mm thickness, OSB 18—OSB samples with 18 mm thickness. Box graphs have X Axis marks as 2—43 kW.m⁻²; 3—44 kW.m⁻²; 4—45 kW.m⁻²; 5—46 kW.m⁻²; 6—47 kW.m⁻²; 7—48 kW.m⁻²; 8—49 kW.m⁻²; and 9—50 kW.m⁻². Confidential interval 95%.

The values of time-to-ignition and mass loss of OSB have a greater dispersion of results, as evidenced by the created box graphs (Figure 5). The variability results from

the nature of the board, which is composed of large-area wood particles from pressed flat chips that are pressed under the influence of high pressure and temperature (Figure 6). The binder is a formaldehyde-based resin [74]. Osvald et al. [75] do not assume the influence of the bonding material (glue as well as other additives) on the thermal degradation of the OSB surface.

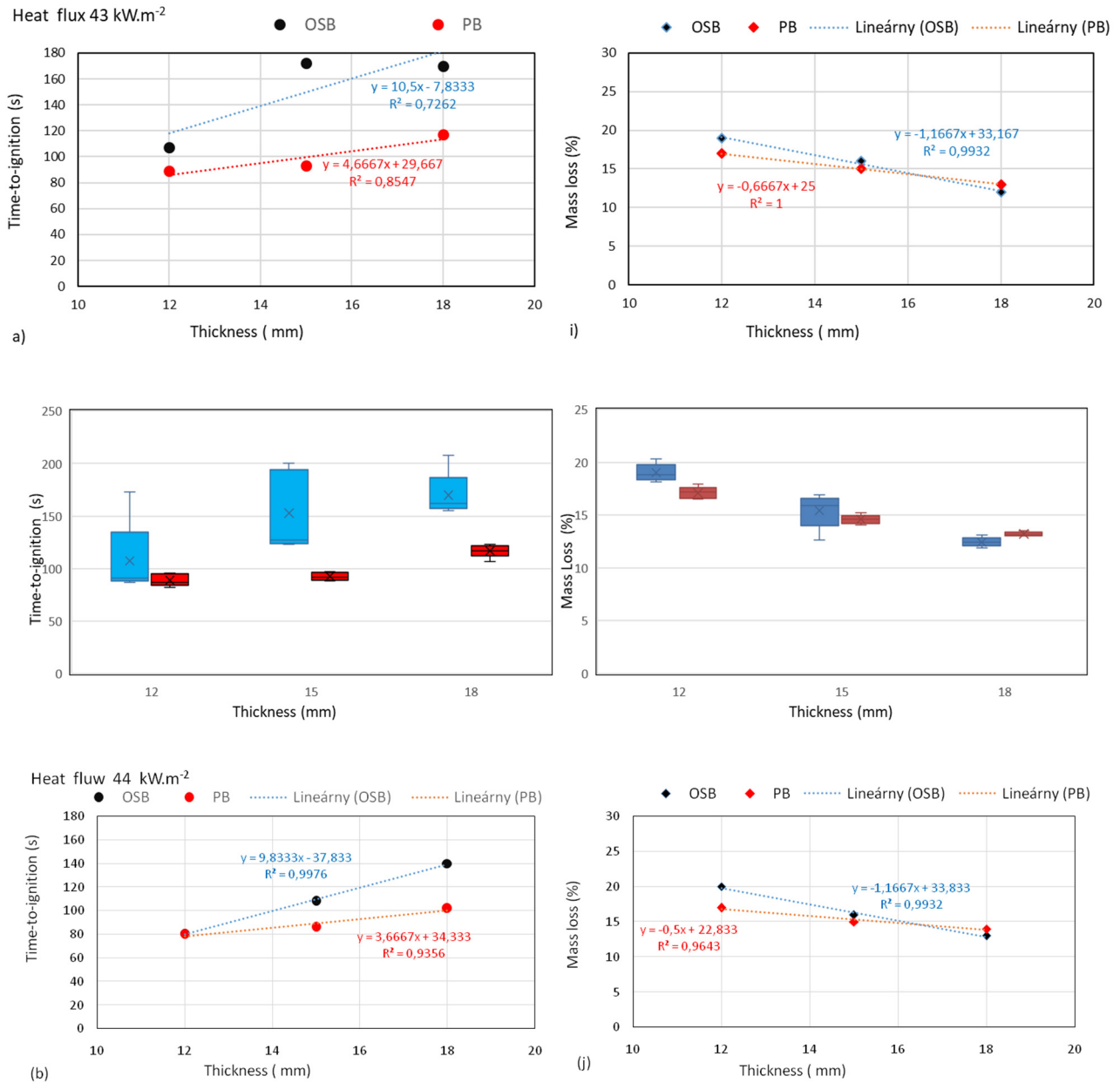


Figure 6. Cont.

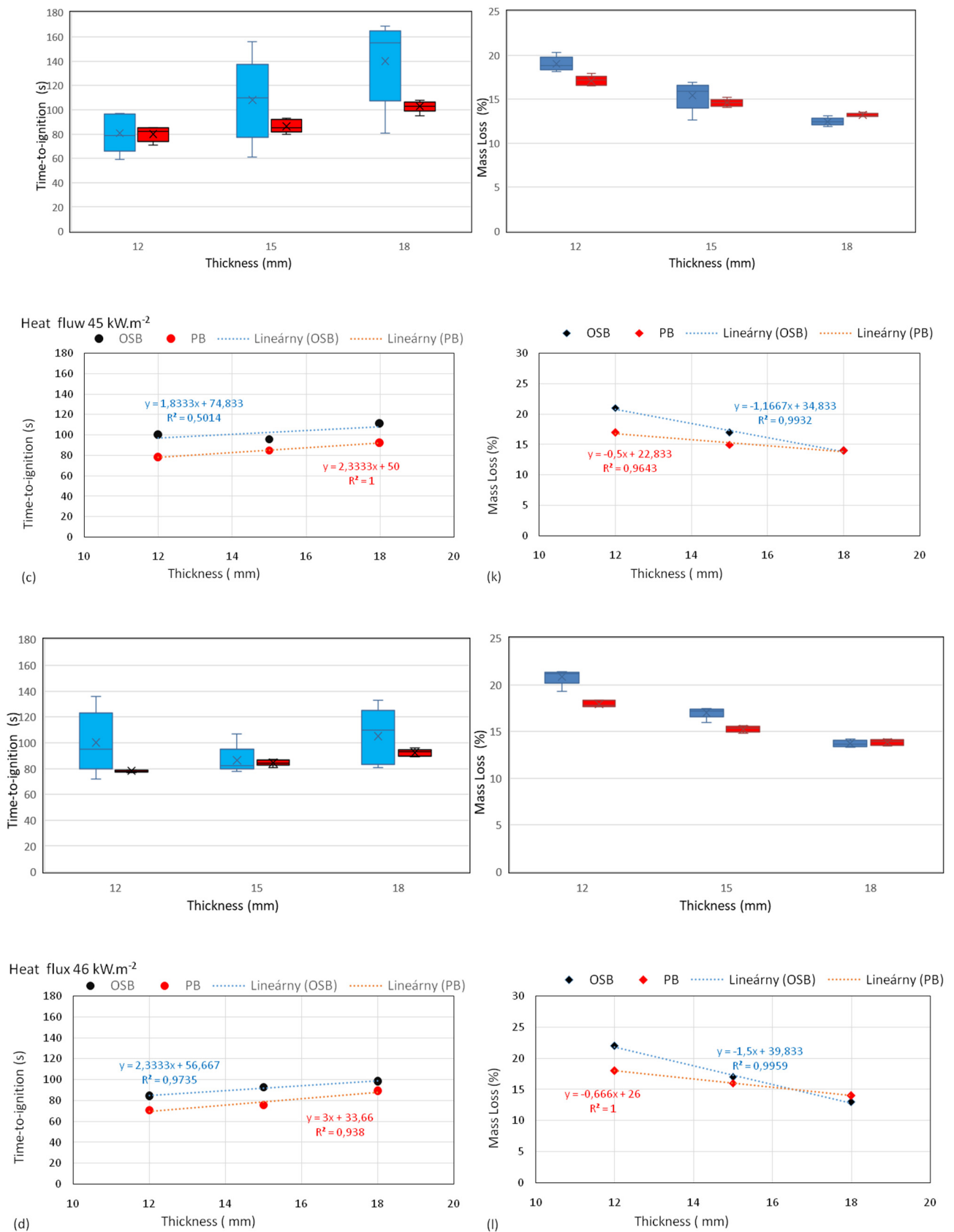


Figure 6. Cont.

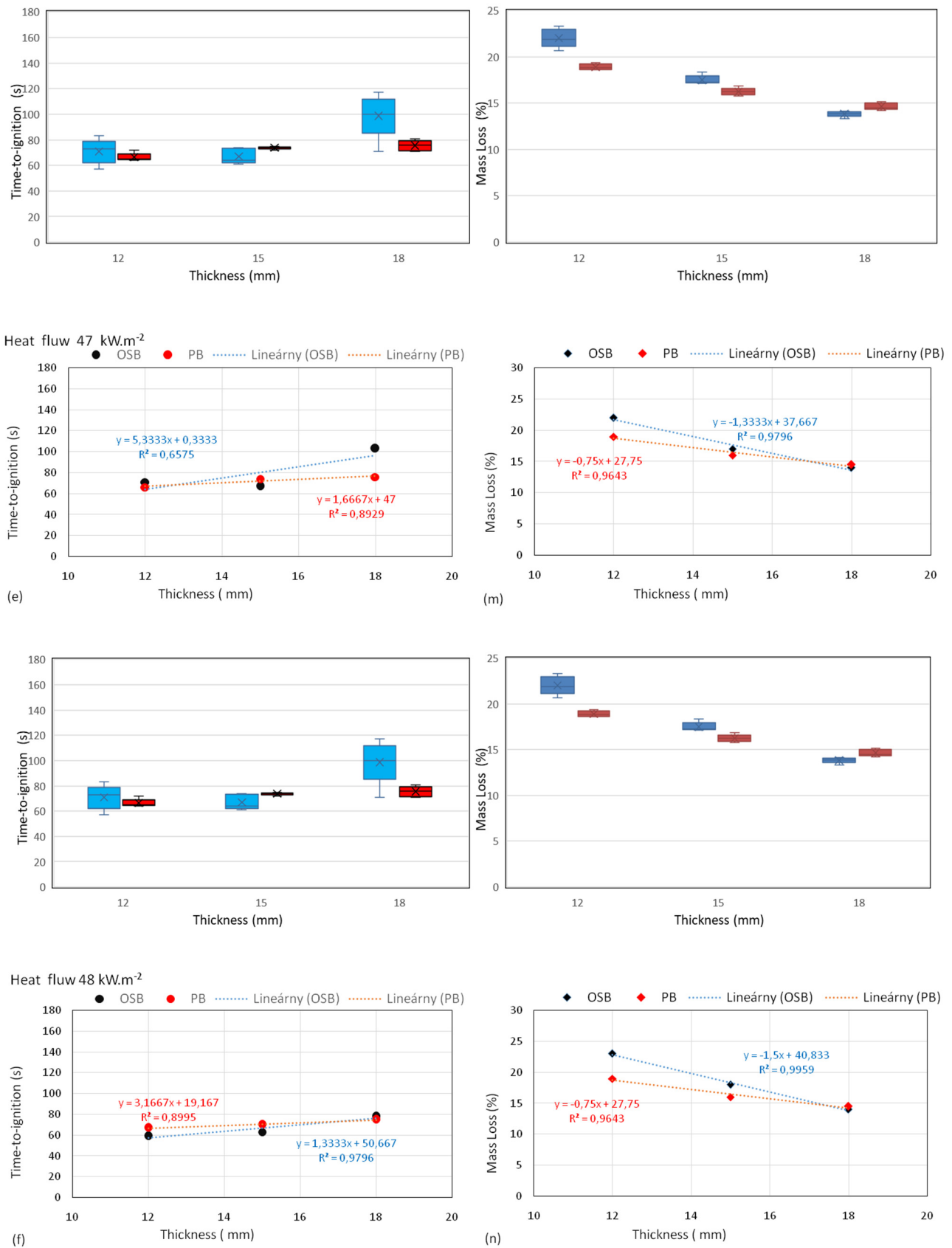


Figure 6. Cont.

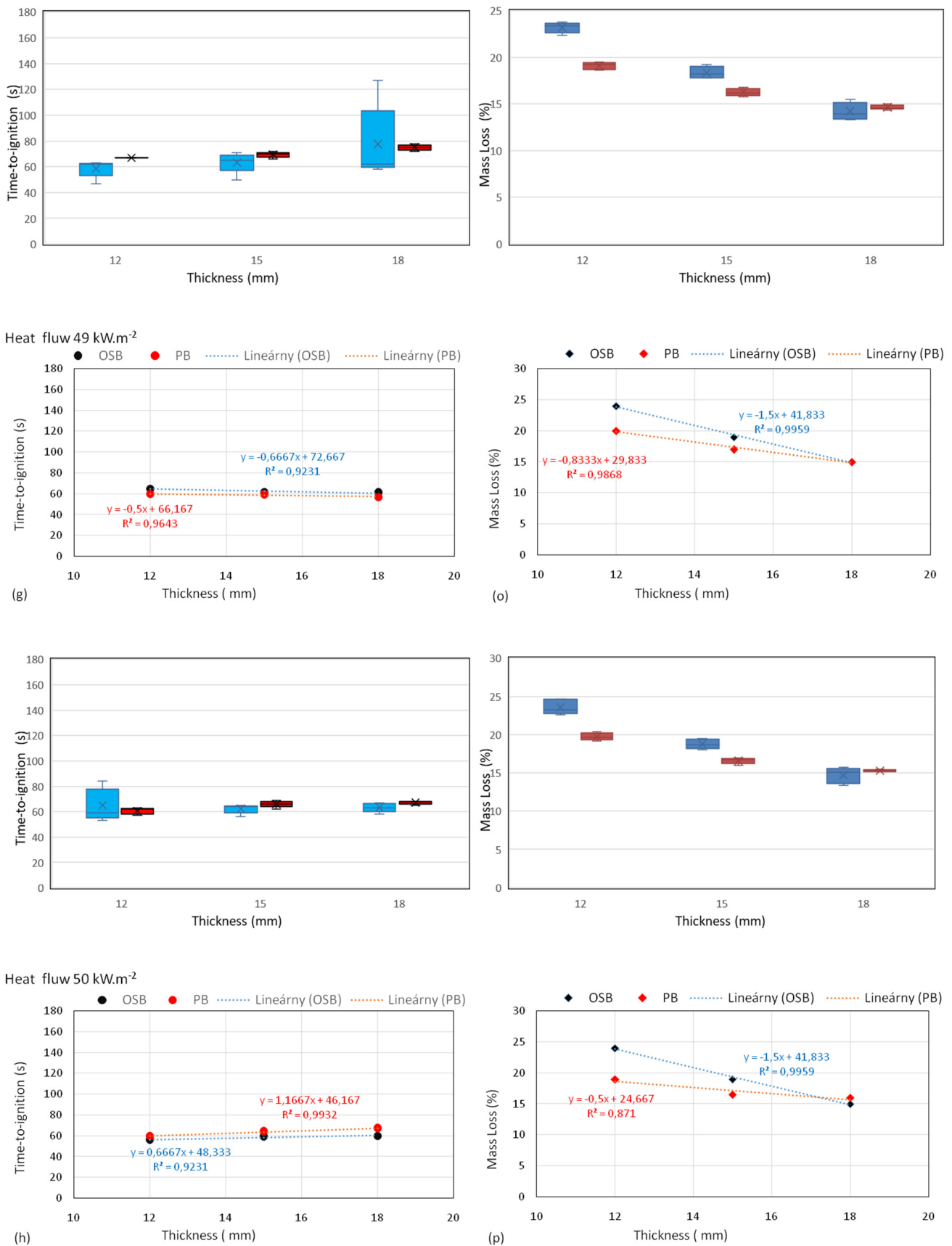


Figure 6. Cont.

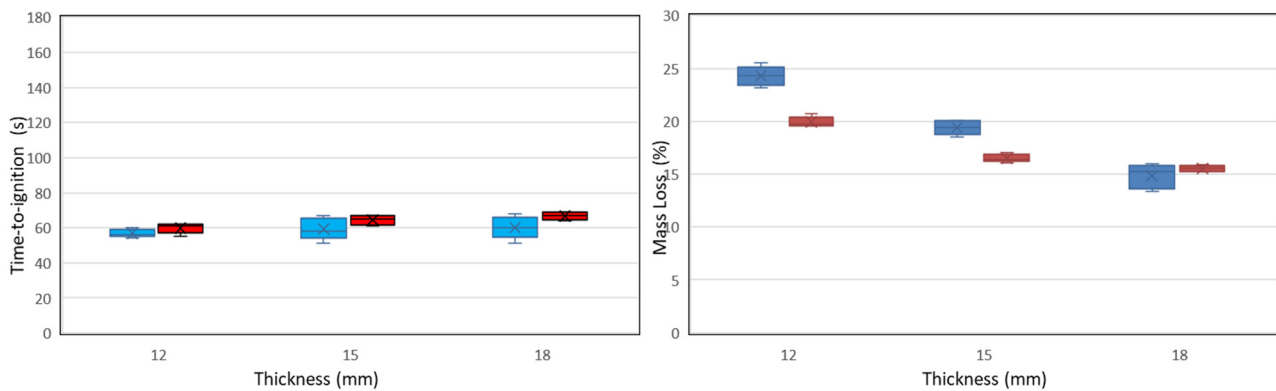


Figure 6. Graphical representation of time-to-ignition and mass loss dependence on board thickness and heat flux with box plots. Legends: blue colour is marked for OSB samples, PB is marked by red, lineárny OSB is linear OSB curve and Lineárny PB is linear curve of PB. Confidential interval 95%.

When comparing the mass loss of particleboards and OSB, lower mass loss values are observed in particleboards of all thicknesses. This difference decreases with increasing sample thickness. Mass loss values of particleboard and OSB samples with a thickness of 18 mm are the same (Figure 5b). A detailed analysis of time-to-ignition and mass loss results for individual sample thicknesses exposed to selected heat flux values is shown in Figure 6. The comparison of time-to-ignition values of particleboards and OSB showed interesting results, apart from the results with the heat flux of $43 \text{ kW}\cdot\text{m}^{-2}$ (Figure 6a). Figure 6 shows the linear dependences of time-to-ignition increase on the sample thickness. At the same time, the graphs are supplemented with quantitative analysis through box graphs. The presented graphs confirm the description of the behaviour of OSB and PB due to the action of radiant heat. Particleboards record lower time-to-ignition values than OSB up to the heat flux of $47 \text{ kW}\cdot\text{m}^{-2}$ (Figure 6b–e). Subsequently, the particleboard and OSB time stamps become identical (Figure 6f–h). All linear dependences maintain an increasing tendency (Figure 6a–h), i.e., the time-to-ignition increases with increasing sample thickness. The given increasing tendency was, however, no longer found at heat flux of 49 and $50 \text{ kW}\cdot\text{m}^{-2}$ (Figure 6g,h).

Naturally, mass loss (Δm) results show the opposite tendency: Δm decreases with increasing sample thickness (Figure 6i–p), while the Δm of OSB is generally greater than the Δm of particleboards. Interesting results can be seen at the heat fluxes of 43 (Figure 6i), 44 (Figure 6j) and 46 (Figure 6l) $\text{kW}\cdot\text{m}^{-2}$, where there is a change in Δm occurring in samples with a thickness of 18 mm. These cases show higher Δm values of particleboard samples compared to OSB.

The results confirm relatively similar behaviour of particleboard and OSB samples. OSB have generally higher time-to-ignition values, i.e., they withstand the effect of radiant heat longer than particleboards. On the other hand, OSB have a higher Δm value compared to particleboards during thermal degradation and subsequent combustion.

Our results show that as the thickness of samples increases, the differences in the behaviour of the samples disappear under action radiant heat, which can be seen in Figure 6. Practice should take into account the importance of thickness when applying these materials in building structures or elements.

For the purpose of this analysis, another parameter evaluating the behaviour of solids in the event of a fire was calculated, namely the burning rate of OSB (Figure 7a) and particleboards (Figure 7b). The process of thermal degradation of wood-based materials is associated with the charring of the surface, hence some authors [49] call this parameter the charring rate. Once again, dependence between the increase in the rate of burning and the increase in heat flux was confirmed. The burning rate ($\text{g}\cdot\text{m}^{-2}\cdot\text{s}^{-1}$) is calculated as the ratio of mass loss Δm to the time of thermal degradation. The results show a decrease in

the rate of burning with increasing thickness of the sample (Figure 8), which is also stated by Richter et al. [49]. This fact confirms that particleboards act as thermal insulators.

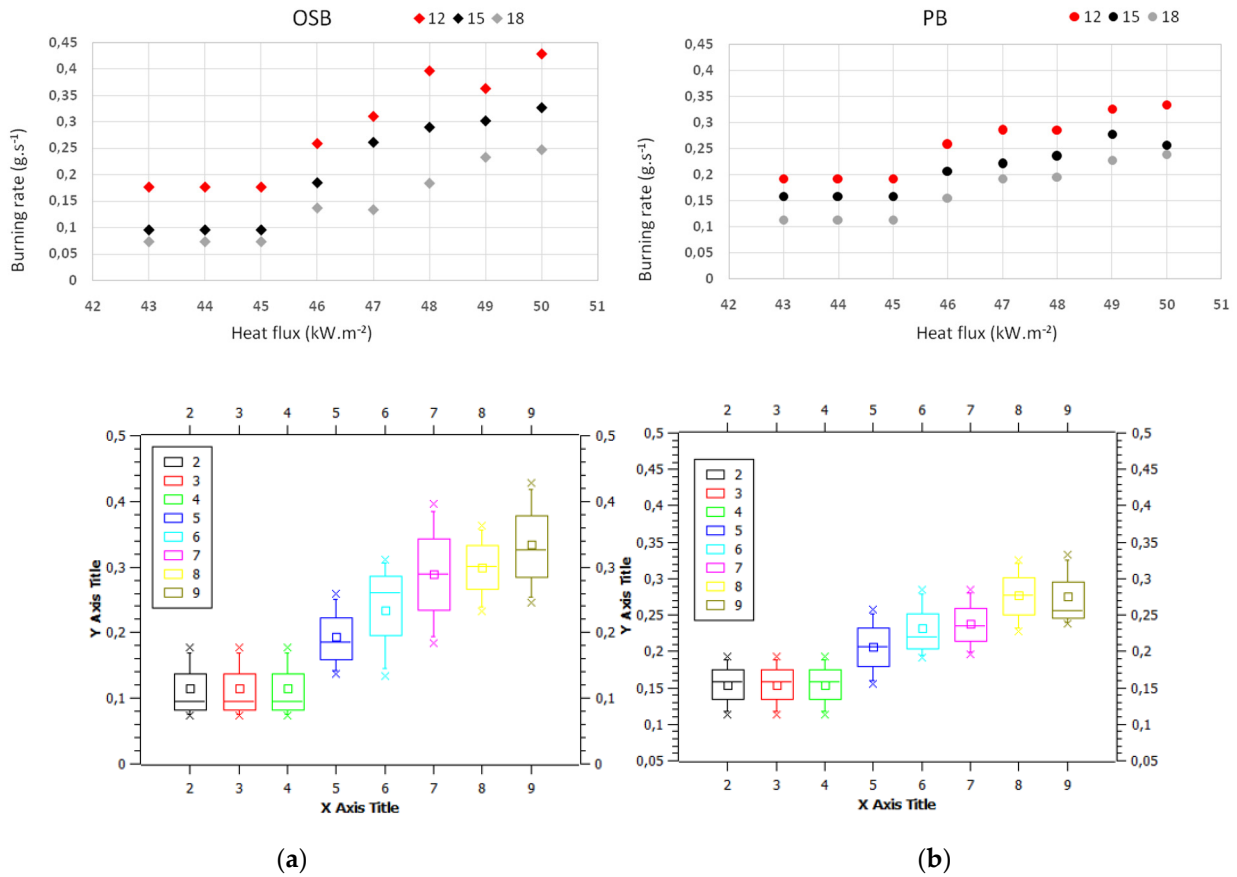


Figure 7. Graphical dependence of burning rate of OSB and PB samples depending on thermal stress. Legend: 12, 15, 18 are values of thickness. Box plots, have X Axis marks as 2—43 kW.m⁻²; 3—44 kW.m⁻²; 4—45 kW.m⁻²; 5—46 kW.m⁻²; 6—47 kW.m⁻²; 7—48 kW.m⁻²; 8—49 kW.m⁻²; and 9—50 kW.m⁻². Confidential interval 95%.

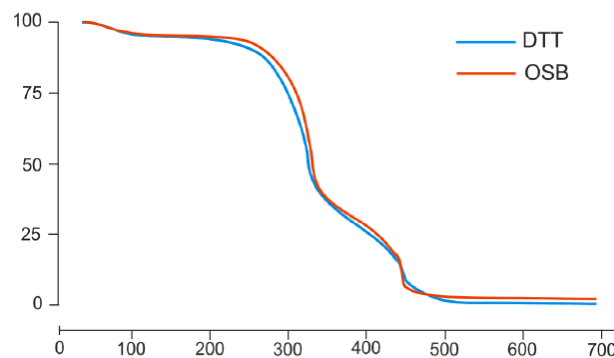


Figure 8. Comparison of thermogravimetric records showing the decomposition of selected board materials at a heating rate of 10 °C.min⁻¹ in an atmosphere of air.

The box plots added to Figure 7 show the same tendency for the burning rate to increase. The values of 43,44, 45 and 46 kW.m⁻² have exactly the same burning rate values, and significant changes occur at heat flows of 48-50 kW.m⁻².

Despite the previous linear dependences, it is not possible to draw a clear conclusion. This fact is also confirmed in Figure 7. The results show a relationship between the thickness of the samples and the burning rate, which is again linear, but the lines differ (Figure 7).

Richter et al. [49] addressed the effect of oxygen concentration and heat flux on the ignition and burning of particleboards. The experiments were performed on samples of particleboards with different oxygen concentrations (0%–21%), heat fluxes (10–70 kW.m⁻²), sample densities (600–800 kg.m⁻²) and sample thicknesses (6–25 mm). The results of Richter et al. [49] showed the effect of heat flux and oxygen concentration on the rate of burning, ignition time and combustion type (pyrolysis, smouldering, combustion).

Maciulaitis et al. [70] watched, among other things, the influence of 30, 35, 40, 45 and 50 kW.m⁻² heat flows in accordance with LST ISO 5657: 1999 [65] with 6 mm, 10 mm, 15 mm and 18 mm thick oriented strand boards (OSBs).

Statistical evaluation of measurement data

The assessment of the impact of the kind samples (PB, OSB) and the impact of thickness (12,15 and 18 mm) on time-to-ignition and mass loss was carried out by statistical analysis. We used the multifactor analysis of variance (ANOVA) using LSD (95% level of provability) of the test (software Statistica 10).

Table 4 confirms significant differences for thickness. The OSB 18 mm has the highest time-to-ignition value.

Table 4. The impact of samples (PB, OSB) and impact of thickness (12.15 and 18 mm) on the time-to-ignition through the 1-factor analysis of variance (ANOVA) ($\alpha = 0.05$).

Samples	Thickness (mm)	Heat Flux (kW.m ⁻¹)								Average	Hd $\alpha_{0.5}$
		43	44	45	46	47	48	49	50		
OSB	12	107.40	80.00	100.2	84.4	71.0	58.6	65.00	56.8	77.9a	
OSB	15	152.80	108.00	86.40	87.2	67.0	63.4	62.2	59.4	85.8b	
OSB	18	170.00	140.00	105.20	98.8	103.6	77.6	63.2	60.2	102.3c	
PB	12	89.00	80.00	78.2	71.6	66.4	67.0	60.6	59.8	71.6a	
PB	15	92.60	86.00	84.4	76.0	73.8	69.4	66.0	64.4	76.6ab	
PB	18	117.00	102.00	92.2	89.0	75.6	75.0	67.2	66.8	85.6b	
Average		121.4e	99.6d	91.1d	84.5c	75.4b	68.5ab	64.0a	61.2a	4.47	

ANOVA–LSD test ($\alpha = 0.05$): a, b, c, d, e—statistically significant difference.

The mass loss for all samples was 15% of the original weight of the samples. The obtained statistical data did not confirm the significance of the influence of the kind of sample and its thickness on mass loss (Table 5).

Table 5. The impact of samples (PB, OSB) and impact of thickness (12.15 and 18 mm) on the time-to-ignition through the 1-factor analysis of variance (ANOVA) ($\alpha = 0.05$).

Samples	Heat Flux (kW.m ⁻¹)								Average	Hd $\alpha_{0.5}$
	43	44	45	46	47	48	49	50		
OSB	15.6	16.5	17.2	17.5	17.7	18.5	19.0	19.5	17.1a	
PB	14.5	15.6	15.7	15.9	16.6	16.7	17.2	17.3	16.1a	
Average	15.2b	16.1a	16.5a	16.8a	17.2a	17.6a	18.1c	18.4c	3.45	

ANOVA–LSD test ($\alpha = 0.05$): a, b, c—statistically significant difference.

Thermal analysis is another method which uses constant heating to analyse the sample. The results confirm thermal decomposition of samples in two stages [49], as is the case with other cellulosic materials (Table 6). Individual stages of thermal decomposition of particleboard and OSB samples were defined with the use of thermogravimetric analysis in an atmosphere of air.

Table 6. Thermogravimetric analysis of OSB and particleboard samples.

Sample	Drying Processes			Thermal Degradation Processes						
	Temperature Range (°C)	Tp (°C)	Δm (%)	I. Stage			II. Stage			
				Temperature Range (°C)	Tp (°C)	Δm (%)	Temperature Range (°C)	Tp (°C)	Δm (%)	C _{rezist} (%)
OSB	42–136	72.3	4.86	179–381	325.7	65.07	381–524	443.0	29.34	0.61
Particleboard	42–136	72.3	5.32	146–378	320.3	64.65	378–525	445.7	29.53	0.64

Thermal decomposition of the OSB sample (Figure 8) took place in two stages. The first stage of thermal decomposition, the main decomposition of the sample, occurred at a temperature of 179 °C. The highest mass loss (65.07%) was recorded at 325.7 °C within the first stage of decomposition, which ranged between the temperature of 179 °C and 381 °C. The second stage of thermal decomposition began at 381 °C. At this stage, the second maximum rate of mass loss was recorded at 443 °C, with a mass loss of 39.34% and a resistant residue of 0.61% after decomposition.

A similar course of thermal degradation was observed in particleboards. The main decomposition of the particleboard sample occurred at a temperature of 146 °C within the temperature range of up to 378 °C. At the same time, the highest mass loss of 64.65% was recorded at the temperature of 320.3 °C. In the second stage of thermal decomposition, which took place at the temperature range of 378 °C to 525 °C, the second maximum rate of mass loss was recorded at 445.7 °C. At this stage, there was a mass loss of 29.53% and the resistant residue after decomposition amounted to 0.64%.

Given values show the behaviour of boards subjected to thermal stress, where the OSB with a thickness of 12 mm begins to thermally degrade at 179 °C and its ignition time is 107 s at a heat flux of 43 kW.m⁻².

Particleboard with the thickness of 12 mm begins to degrade at 146 °C and its ignition time is 89 s. The reported results are consistent in all sample thicknesses and heat flux values.

Sinha et al. [76] studied the effect of exposure time on the flexural strength of OSB and plywood at elevated temperatures. They reached a critical temperature of 190 °C at which the strength decreased and thermal degradation occurred. Very interesting research on time-to-ignition on Ancient Wood was conducted by Wang et al. [77].

4. Conclusions

Based on the performed experiments, it is possible to draw the following conclusions:

1. The heat flux and thickness had a significant effect only on time-to-ignition.
2. OSB had a higher time-to-ignition than particleboards and the thermal degradation of OSB started later, i.e., at a higher temperature than that of particleboards. Above 47 kW.m⁻², the samples yielded the same results, but OSB had a higher mass loss value than particleboards.
3. Thermal analysis also confirmed a higher thermal decomposition temperature of OSB (179 °C) compared to particleboards (146 °C). The difference in mass loss in both stages did not exceed 1%, and other parameters did not show a significant difference in the behaviour of the samples.
4. Our results show that as the thickness samples increases, the differences in the behaviour of the samples disappear under action radiant heat, which can be seen in Figure 6. Practice should take into account the importance of thickness when applying these materials in building structures or elements.

Author Contributions: Conceptualization, I.T. and M.I.; methodology, I.T.; software, I.M.; validation, I.T., M.I. and J.H.; formal analysis, I.T. and L.M.O.; investigation, I.T. and M.I.; resources, I.T., J.H. and M.I.; data curation, M.I.; writing—original draft preparation, I.T.; writing—review and editing, I.M. and I.T.; project administration, L.M.O.; funding acquisition, I.T. All authors have read and agreed to the published version of the manuscript.

Funding: This article was supported by Institute Grant of University of Žilina No. 12716 and the Cultural and Educational Grant Agency of the Ministry of Education, Science, Research and Sport of the Slovak Republic on the basis of the project KEGA 0014UKF-4/2020 Innovative Learning e-modules for Safety in Dual education.

Informed Consent Statement: Not applicable.

Data Availability Statement: Not applicable for studies not involving humans or animals.

Acknowledgments: This article was supported by the Institute Grant of University of Žilina No. 12716 and Project KEGA 0014UKF-4/2020 Innovative Learning e-modules for Safety in Dual Education.

Conflicts of Interest: The authors declare no conflict of interest.

References

1. Mantanis, G.I.; Athanassiadou, E.T.; Barbu, M.C.; Wijnendaele, K. Adhesive systems used in the European particleboard, MDF and OSB industries. *Wood Mater. Sci. Eng.* **2007**, *13*, 104–116. [[CrossRef](#)]
2. Pedzik, M.; Auriga, R.; Rogozinski, T. Physical and Mechanical Properties of Particleboard Produced with Addition of Walnut (*Juglansregia L.*) Wood Residues. *Materials* **2022**, *15*, 1280. [[CrossRef](#)] [[PubMed](#)]
3. Ligne, L.D.; Van Acker, J.; Baetens, J.M.; Omar, S.; De Baets, B.; Thygesen, L.G.; Van Den Bulcke, J.; Thybring, E.E. Moisture dynamics of wood-based panels and wood fibre insulation materials. *Front. Plant Sci. Sec. Plant Biophys. Model.* **2022**, *13*, 951175. [[CrossRef](#)] [[PubMed](#)]
4. Seng, H.L.; Lum, W.C.; Boon, J.G.; Kristak, L.; Antov, P.; Peđzik, M.; Rogoziński, T.; Taghiyari, H.R.; Lubis, M.A.R.; Fatriasari, W.; et al. Particleboard from agricultural biomass and recycled wood waste: A review. *J. Mater. Res. Technol.* **2022**, *20*, 4630–4658. [[CrossRef](#)]
5. Hellmeister, V.; Barbirato, G.H.A.; Lopes, W.E.; dos Santos, V.; Fiorelli, J. Evaluation of Balsa wood (*Ochromapyramidale*) waste and OSB panels with castor oil polyurethane resin. *Int. Wood Prod. J.* **2021**, *12*, 267–276. [[CrossRef](#)]
6. Bušterová, M. *Effect of Heat Flux on the Ignition of Selected Board Materials*; Faculty of Materials Science and Technology in Trnava, Slovak University of Technology in Bratislava: Bratislava, Slovakia, 2011; p. 149.
7. Makowski, M.; Ohlmeyer, M. Impact of drying temperature and pressing time factor on VOC emissions from OSB made of Scots pine. *Holzforschung* **2006**, *60*, 417–422. [[CrossRef](#)]
8. Boruszewski, P.; Borysiuk, P.; Jankowska, A.; Pazik, J. Low-Density Particleboards Modified with Blowing Agents-Characteristic and Properties. *Materials* **2022**, *15*, 4528. [[CrossRef](#)]
9. Adamová, T.; Hradecký, J.; Pánek, M. Volatile Organic Compounds (VOCs) from Wood and Wood-Based Panels: Methods for Evaluation, Potential Health Risks, and Mitigation. *Polymers* **2020**, *12*, 2289. [[CrossRef](#)] [[PubMed](#)]
10. Copak, A.; Jirouš-Rajković, V.; Španić, N.; Miklečić, J. The Impact of Post-Manufacture Treatments on the Surface Characteristics Important for Finishing of OSB and Particleboard. *Forests* **2021**, *12*, 975. [[CrossRef](#)]
11. Bekhta, P.; Noshchenko, G.; Reh, R.; Kristak, L.; Antov, P.; Mirski, R. Properties of eco-friendly particleboards bonded with lignosulfonate-urea-formaldehyde adhesives and PMDI as a crosslinker. *Materials* **2021**, *14*, 4875. [[CrossRef](#)]
12. Krišťák, L.; Réh, R. Application of Wood Composites. *Appl. Sci.* **2021**, *11*, 3479. [[CrossRef](#)]
13. Mirski, R.; Derkowski, A.; Dziurka, D. Dimensional stability of OSB panels subjected to variable relative humidity: Core layer made with fine wood chips. *BioResources* **2013**, *8*, 6448–6459. [[CrossRef](#)]
14. Gaff, M.; Kacik, F.; Gasparik, M. The effect of synthetic and natural fire-retardants on burning and chemical characteristics of thermally modified teak (*Tectonagrandis L. f.*) wood. *Constr. Build. Mater.* **2019**, *200*, 551–558. [[CrossRef](#)]
15. Wang, S.Q.; Gu, H.M.; Wang, S.G. Layer thickness swell and related properties of commercial OSB products: A comparative study. In Proceedings of the 37th International Wood Composite Materials Symposium Proceedings, Pullman, WA, 7–10 April 2003; pp. 65–76.
16. Georgescu, S.-V.; Şova, D.; Campean, M.; Coşoreanu, C. A Sustainable Approach to Build Insulated External Timber Frame Walls for Passive Houses Using Natural and Waste Materials. *Forests* **2022**, *13*, 522. [[CrossRef](#)]
17. Salem, M.Z.M.; Böhm, M.; Šedivka, P.; Nasser, R.A.; Ali, H.M.; Abo Elgat, W.A.A. Some physico-mechanical characteristics of uncoated OSB ECO-products made from Scots pine (*Pinussylvestris L.*) and bonded with PMDI resin. *BioResources* **2018**, *13*, 1814–1828. [[CrossRef](#)]
18. Paes, J.B.; Maffioletti, F.D.; Lahr, F.A.R. Biological resistance of sandwich particleboard made with sugarcane, thermally-treated Pinus wood and malva fiber. *J. Wood Chem. Technol.* **2022**, *42*, 171–180. [[CrossRef](#)]
19. Kup, F.; Vural, C. Determination of physical and mechanical properties of particleboard obtained from cotton and corn stubble with fibreglass plaster net. *J. Environ. Prot. Ecol.* **2022**, *23*, 657–667.
20. Zheng, N.H.; Wu, D.N.; Sun, P.; Liu, H.G.; Luo, B.; Li, L. Mechanical Properties and Fire Resistance of Magnesium-Cemented Poplar Particleboard. *Materials* **2020**, *13*, 115. [[CrossRef](#)]
21. Han, G.P.; Wu, Q.L.; Lu, J.Z. Selected properties of wood strand and oriented strandboard from small-diameter southern pine trees. *Wood Fiber Sci.* **2006**, *36*, 621–632.

22. Makovická Osvaldová, L.; Mitrenga, M.; Jancík, J.; Titko, M.; Efhamisisi, D.; Košútová, K. Fire Behaviour of Treated Insulation Fibreboards and Predictions of its Future Development Based on Natural Aging Simulation. *Front. Mater.* **2022**, *9*, 891167. [[CrossRef](#)]
23. Efe, F.T. Investigation of some physical and thermal insulation properties of honeycomb-designed panels produced from Calabrian pine bark and cones. *Eur. J. Wood Wood Prod.* **2022**, *80*, 705–718. [[CrossRef](#)]
24. Malý, S.; Vavrečková, K.; Malme, K.; Kubás, J.; Hollá, K.; Makovická Osvaldová, L. Occupational Health and Safety of Food Industry Employees with Emphasis on Specific Diseases. In *Innovation Management and Sustainable Economic Development in the Era of Global Pandemic, Proceedings of the 38th International Business Information Management Association Conference, IBIMA Publishing, Seville, Spain, 23–24 November 2021*; IBIMA Publishing: Seville, Spain, 2021; ISBN 978-0-9998551-7-1. ISSN 2767-9640.
25. Ramos, A.; Briga-Sa, A.; Pereira, S.; Correia, M.; Pinto, J.; Bentes, I.; Teixeira, C.A. Thermal performance and life cycle assessment of corn cob particleboards. *Build. Eng.* **2021**, *44*, 102998. [[CrossRef](#)]
26. Górski, J.; Podziewski, P.; Borysiuk, P. The Machinability of Flat-Pressed, Single-Layer Wood-Plastic Particleboards while Drilling—Experimental Study of the Impact of the Type of Plastic Used. *Forests* **2022**, *13*, 584. [[CrossRef](#)]
27. Langová, N.; Réh, R.; Igaz, R.; Krišťák, L.; Hitka, M.; Joščák, P. Construction of wood-based lamella for increased load on seating furniture. *Forests* **2019**, *10*, 525. [[CrossRef](#)]
28. Tabarsi, E.; Kozak, R.; Cohen, D.; Gaston, C. A market assessment of the potential for OSB products in the North American office furniture and door manufacturing industries. *For. Prod. J.* **2003**, *53*, 19–27.
29. Zamarian, E.H.C.; Iwakiri, S.; Trianoski, R.; de Albuquerque, C.E.C. Production of particleboard from discarded furniture. *Rev. Arvore* **2013**, *41*, 410407. [[CrossRef](#)]
30. Réh, R.; Krišťák, L.; Sedliachik, J.; Bekhta, P.; Božiková, M.; Kunecová, D.; Vozárová, V.; Tudor, E.M.; Antov, P.; Savov, V. Utilization of Birch Bark as an Eco-Friendly Filler in Urea-Formaldehyde Adhesives for Plywood Manufacturing. *Polymers* **2021**, *13*, 511. [[CrossRef](#)]
31. Eickner, H.W. Fire resistance of solid-core wood flush doors. *For. Prod. J.* **1976**, *23*, 38–43.
32. Harada, K. A review on structural fire resistance. In *Proceedings of the Fourth Asia-Oceania Symposium on Fire Science & Technology*, Tokyo, Japan, 24–26 May 2000; Asia-Oceania Association for Fire Science & Technology/Japan Association for Fire Science & Engineering: Tokyo, Japan, 2000; pp. 155–163.
33. White, R.H. Fire resistance of exposed wood members. In *Proceedings of the Wood & Fire Safety: Proceedings, 5th International Scientific Conference*, Zvolen, Slovakia., 18–22 April 2004; Tech. University of Zvolen: Zvolen, Slovakia.
34. Ayrlimis, N.; Kartal, S.; Laufenberg, T.; Winandy, J.; White, R. Physical and mechanical properties and fire, decay, and termite resistance of treated oriented strandboard. *For. Prod. J.* **2005**, *55*, 74.
35. Östman, B.A.L.; Mikkola, E. European classes for the reaction to fire performance of wood products. *HolzalsRoh Und Werkst.* **2006**, *64*, 327–337. [[CrossRef](#)]
36. Tudor, E.M.; Scheriau, C.; Barbu, M.C.; Réh, R.; Krišťák, L.; Schnabel, T. Enhanced resistance to fire of the bark-based panels bonded with clay. *Appl. Sci.* **2020**, *10*, 5594. [[CrossRef](#)]
37. Salek, V.; Cabova, K.; Wald, F.; Jahoda, M. Numerical modelling of fire test with timber fire protection. *J. Struct. Fire Eng.* **2022**, *13*, 99–117. [[CrossRef](#)]
38. Rantuch, P. Comparing the Ignition Parameters of Various Polymers. In *Ignition of Polymers. Springer Series on Polymer and Composite Materials*; Springer: Cham, Switzerland, 2021. [[CrossRef](#)]
39. Liu, Y.T. Cone Calorimeter Analysis on the Fire-resistant Properties of FRW Fire-retardant Particleboard. *Adv. Mater. Process.* **2011**, *311*, 2142–2145.
40. Turkowski, P.; Węgrzyński, W. Comparison of a Standard Fire-Resistance Test of a Combustible Wall Assembly with Experiments Employing Pre-defined Heat Release Curves. *Fire Technol.* **2022**, *58*, 1767–1787. [[CrossRef](#)]
41. Baranovskii, N.V.; Kirienko, V.A. Ignition of Forest Combustible Materials in a High-Temperature Medium. *J. Eng. Phys.* **2020**, *93*, 1266–1271. [[CrossRef](#)]
42. Kristak, L.; Ruziak, I.; Tudor, E.M.; Barbu, M.C.; Kain, G.; Reh, R. Thermophysical properties of larch bark composite panels. *Polymers* **2021**, *13*, 2287. [[CrossRef](#)]
43. Madyaratri, E.W.; Ridho, M.R.; Aristri, M.A.; Lubis, M.A.R.; Iswanto, A.H.; Nawawi, D.S.; Antov, P.; Kristak, L.; Majlingová, A.; Fatriasari, W. Recent Advances in the Development of Fire-Resistant Biocomposites—A Review. *Polymers* **2022**, *14*, 362. [[CrossRef](#)]
44. Rybinski, P.; Syrek, B.; Szwed, M.; Bradlo, D.; Zukowski, W.; Marzec, A.; Sliwka-Kaszynska, M. Influence of Thermal Decomposition of Wood and Wood-Based Materials on the State of the Atmospheric Air. Emissions of Toxic Compounds and Greenhouse Gases. *Energies* **2021**, *14*, 3247. [[CrossRef](#)]
45. Gong, J.H.; Zhou, H.G.; Zhu, H.; McCoy, C.G.; Stoliarov, S.I. Development of a pyrolysis model for oriented strand board: Part II—Thermal transport parameterization and bench-scale validation. *J. Fire Sci.* **2021**, *39*, 477–494. [[CrossRef](#)]
46. Diertenberger, M.A.; Shalbfan, A.; Welling, J. Cone calorimeter testing of foam core sandwich panels treated with intumescent paper underneath the veneer (FRV). *Fire Mater.* **2018**, *42*, 296–305. [[CrossRef](#)]
47. Mikkola, E.; Wichman, I.S. On the thermal ignition of combustible materials. *Fire Mater.* **1989**, *14*, 87–96. [[CrossRef](#)]
48. Hao, H.; Chow, C.L.; Lau, D. Effect of heat flux on combustion of different wood species. *Fuel* **2020**, *278*, 118325. [[CrossRef](#)]
49. Richter, F.; Jervis, F.X.; Huang, X.Y.; Rein, G. Effect of oxygen on the burning rate of wood. *Combust. Flame* **2021**, *234*, 111591. [[CrossRef](#)]

50. Renner, J.S.; Mensah, R.A.; Jiang, L.; Xu, Q.; Das, O.; Berto, F. Fire Behavior of Wood-Based Composite Materials. *Polymers* **2022**, *13*, 4352. [[CrossRef](#)] [[PubMed](#)]
51. Kuracina, R.; Szabova, Z.; Bachraty, M.; Mynarz, M.; Skvarka, M. A new 365-litre dust explosion chamber: Design and testing. *Powder Technol.* **2021**, *386*, 420–427. [[CrossRef](#)]
52. Rantuch, P.; Hrusovsky, I.; Martinka, J.; Balog, K. Calculation of critical heat flux for ignition of oriented strand boards. *Fire Prot. Saf. Secur.* **2017**, *207*, 214–222.
53. *CEN Standard EN ISO 13943: 2018; Fire safety. Vocabulary.* European Committee for Standardization: Brussels, Belgium, 2018.
54. *ISO 3261:1975; Fire tests—Vocabulary.* International Organization for Standardization: Geneva, Switzerland, 1995.
55. Rantuch, P.; Kaciková, D.; Martinka, J.; Balog, K. The Influence of Heat Flux Density on the Thermal Decomposition of OSB. *Acta Facultatis Xylologiae Zvolen res Publica Slovaca* **2015**, *57*, 125–134.
56. Babrauskas, V. Ignition of wood. A Review of the State of the Art. In *Interflam 2001*; Interscience Communications Ltd.: London, UK, 2001; pp. 71–88.
57. Babrauskas, V. *Ignition Handbook*, 1st ed.; Fire Science Publishers: Issaquah, WA, USA, 2003.
58. Babrauskas, V. Charring rate of wood as a tool for fire investigations. *Fire Saf. J.* **2005**, *40*, 528–554. [[CrossRef](#)]
59. Baranovskiy, N.V.; Kirienko, V.A. Mathematical Simulation of Forest Fuel Pyrolysis and Crown Forest Fire Impact for Forest Fire Danger and Risk Assessment. *Processes* **2022**, *10*, 483. [[CrossRef](#)]
60. Janssens, M.L. Modeling of the thermal degradation of structural wood members exposed to fire. In *Second International Workshop on “Structures in Fire” (SiF ‘02)*; Department of Civil Engineering, University of Canterbury: Christchurch, New Zealand, 2002; pp. 211–222.
61. Chen, X.J.; Yang, L.Z.; Ji, J.W.; Deng, Z.H. Mathematical model for prediction of pyrolysis and ignition of wood under external heat flux. *Prog. Nat. Sci. Mater. Int.* **2002**, *12*, 874–877.
62. Reszka, P.; Borowiec, P.; Steinhaus, T.; Torero, J.L. A methodology for the estimation of ignition delay times in forest fire modelling. *Combust. Flame* **2012**, *159*, 3652–3657. [[CrossRef](#)]
63. Technical and Safety Data Sheet. *Boards Made of Oriented Flat Triples without Surface Treatment—OSB SUPERFINISH ECO, Type OSB/3*; Bučina DDD: Zvolen, Slovakia, 2019.
64. Safety data sheet Particleboard. In *Raw Un-Sanded*; Bučina DDD: Zvolen, Slovak republic, 2019.
65. *ISO 5657:1997; Reaction to Fire Tests—Ignitability of Building Products using a Radiant Heat Source.* International Organization for Standardization: Geneva, Switzerland, 1997.
66. Božiková, M.; Kotoulek, P.; Bilčík, M.; Kubík, L.; Hlaváčová, Z.; Hlaváč, P. Thermal properties of wood and wood composites made from wood waste. *Int. Agrophys.* **2021**, *35*, 251–256. [[CrossRef](#)]
67. *EN 323:1993; Wood-Based Panels—Determination of Density.* European Committee for Standardization: Brussels, Belgium, 1993.
68. Turekova, I.; Markova, I.; Ivanovicova, M.; Harangozo, J. Experimental Study of Oriented Strand Board Ignition by Radiant Heat Fluxes. *Polymers* **2021**, *13*, 709. [[CrossRef](#)] [[PubMed](#)]
69. Turekova, I.; Ivanovicova, M.; Harangozo, J.; Gaspercova, S.; Markova, I. Experimental Study of the Influence of Selected Factors on the Particle Board Ignition by Radiant Heat Flux. *Polymers* **2022**, *14*, 1648. [[CrossRef](#)] [[PubMed](#)]
70. Maciulaitis, R.; Praniauskas, V.; Yakovlev, G. Research into the fire properties of wood products most frequently used in construction. *J. Civ. Eng. Manag.* **2013**, *19*, 573–582. [[CrossRef](#)]
71. Hakkarainen, T. Rate of heat release and ignitability indices in predicting SBI test results. *J. Fire Sci.* **2001**, *19*, 284–305. [[CrossRef](#)]
72. Kucera, P.; Lokaj, A.; Vicek, V. Behavior of the Spruce and Birch Wood from the Fire Safety Point of View. MATERIALS, MECHANICAL AND MANUFACTURING ENGINEERING. *Book Ser. Adv. Mater. Res.* **2014**, *842*, 725. [[CrossRef](#)]
73. Fagbemi, O.D.; Andrew, J.E.; Sithole, B. Beneficiation of wood sawdust into cellulose nanocrystals for application as a bio-binder in the manufacture of particleboard. *Biomass Conv. Bioref.* **2021**, 1–12. [[CrossRef](#)]
74. Michalovič, R. Assessment of different floors materials from the point of view of fire safety. In *Proceedings of the 19th International Scientific Conference Solving Crisis Situations in a Specific Environment*, Faculty of Security Engineering University of Žilina, Žilina, Slovakia, 21–22 May 2014; pp. 497–504.
75. Osvald, A.; Tereňová, L.; Štefková, J. The Impact of Radiant Heat on Flexural Strength and Impact Toughness in OSB Panels. *Delta* **2020**, *14*, 26–35. [[CrossRef](#)]
76. Sinha, A.; Nairn, J.A.; Gupta, R. Thermal degradation of bending strength of plywood and oriented strand board: A kinetics approach. *Wood Sci. Technol.* **2021**, *45*, 315–330. [[CrossRef](#)]
77. Wang, Y.; Wang, W.; Zhou, H.; Qi, F. Burning Characteristics of Ancient Wood from Traditional Buildings in Shanxi Province, China. *Forests* **2022**, *13*, 190. [[CrossRef](#)]